Proceedings of the 2006 IASME/WSEAS International Conference on Continuum Mechanics, Chalkida, Greece, May 11-13, 2006 (pp85-90)

A hyper-viscosity numerical method for the interaction of a shear-dependent fluid with a rigid body

JOÃO JANELA
Inst. Sup. Economia e Gestão
Dept. Matemática and CEMAT/IST
R. Quelhas, 6, 1200 Lisboa
PORTUGAL

ADÉLIA SEQUEIRA
Inst. Superior Técnico
Dept. Matemática and CEMAT
Av. Rovisco Pais, 1049 Lisboa
PORTUGAL

FERNANDO CARAPAU
Universidade de Évora
Dept. Matemática and CIMA-UE
R. Romão Ramalho, 7000 Évora
PORTUGAL

Abstract: We present a numerical method for the simulation of the motion of rigid bodies in incompressible generalized Newtonian fluids. This work is motivated by the study of some physiological phenomena occurring in the human cardiovascular system where the bodies may be blood particles, clots or valves that we assume to be rigid. This new method is based on a variational formulation on the whole fluid/solid domain introducing constraints that enforce the rigid motion of the bodies. The core of this method consists in relaxing the constraints by introducing a penalty parameter (hyper-viscosity). The convergence to the solution of the relaxed problem is established. Finally we present some numerical results using a common benchmark for this type of problems.

Key–Words: Constrained minimization, hyper-viscosity method, fluid-rigid body interaction, shear-thinning fluid

1 Introduction

The theoretical and numerical study of fluid–rigid body interactions is of major importance in many industrial and biological processes. For example the settling and lift–off of particles is crucial in channel flows in the petroleum and coal industries ([3]). However, in this paper we focus our attention on biomedical applications. The study of blood circulation in the human cardiovascular system can involve interaction problems of blood flow with valves (see [5]), blood clots or a number of suspended particles. For this reason we look for a model that reflects some of the rheological properties of blood and allows to consider some of these interaction problems. Blood is a complex mixture consisting of many different particles (erythrocytes, leukocytes, platelets and other matter) suspended in an aqueous polymer solution, the plasma (Newtonian fluid). These suspended particles, consisting mostly of erythrocytes (red blood cells) form about 45% of the volume of normal human blood and their effect should not be ignored. However, in large and medium vessels blood is usually modelled as a Newtonian liquid but in smaller vessels, with diameters comparable with those of the cells, blood behaves as a shear-thinning fluid. In particular at rest or at low shear rates, it is experimentally observed that blood has a high apparent viscosity (due to erythrocytes aggregation into clusters called *rouleaux*) while at high shear rates the cells become disaggregated and deform into an infinite variety of shapes without changing volume, resulting in a reduction of blood viscosity. Moreover since blood cells are essentially elastic membrane filled with fluid, it seems reasonable to expect blood to behave like a viscoelastic fluid, at least under certain conditions. The shear-thinning viscosity reduces velocity and increases shear rate in regions of constant shear stress while the viscoelasticity amplifies the effect of normal stresses in regions of constant shear-stress (see e.g. [6]). It is commonly accepted that, in blood flow modelling, the shear-thinning effect is dominant and viscoelasticity can be disregarded in a first approach. In this work we consider shear-thinning generalized Newtonian fluids.

Numerical simulations of fluid-rigid body interactions can be carried out in different ways, roughly divided in two main classes. The first one involves a moving mesh following the moving part of the domain. In the second approach the whole computational domain is covered by a static mesh, leading to *fictitious domain* or *embedded domain* methods that make use of Lagrange multipliers to enforce the velocity in the solid phase. The method we propose falls into the second class, using a penalty operator instead of Lagrange multipliers.

2 Continuous problem

For simplicity we consider a connected, bounded and regular domain $\mathcal{O} \subset \mathbb{R}^2$ and define B as a multiply connected regular set such that $B \subset \mathcal{O}$.

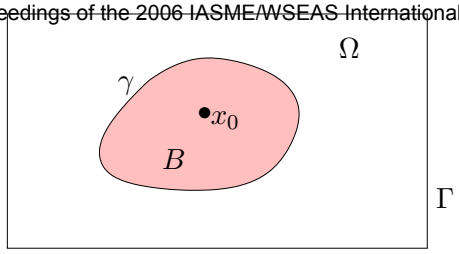

Figure 1: Model domain

We assume that, at time $t \geq 0$, $\Omega = \mathcal{O} - \overline{B}$ is filled with a fluid and B is a rigid inclusion (particle or particles) in $\mathcal{O}$. We denote by Γ the boundary of $\mathcal{O}$ and by γ the boundary of B. Since the position of B is likely to vary over time, these sets will be referred to as B_t and Ω_t.

2.1 Fluid motion

The conservation of linear momentum for the motion of a fluid with velocity $\boldsymbol{u}$ in Ω_t is given by

$$\rho_f \frac{D\boldsymbol{u}}{Dt} = \nabla \cdot \boldsymbol{\sigma} + \boldsymbol{f}_f, \qquad \text{in } \Omega_t \tag{1}$$

where ρ_f is the constant density, $\boldsymbol{f}_f$ the external body forces per unit volume (e.g. gravity), $D\boldsymbol{u}/Dt := \partial_t \boldsymbol{u} + \boldsymbol{u} \cdot \nabla \boldsymbol{u}$ is the material time derivative of $\boldsymbol{u}$ and $\boldsymbol{\sigma}$ is the Cauchy stress tensor. We also assume the incompressibility of the fluid and as a consequence the conservation of mass reduces to

$$\nabla \cdot \boldsymbol{u} = 0, \qquad \text{in } \Omega_t \tag{2}$$

The Cauchy stress tensor for incompressible fluids can be split in terms of the hydrostatic pressure p and the extra stress tensor $\boldsymbol{\tau}$, i.e.

$$\boldsymbol{\sigma} = -p\mathbf{I} + \boldsymbol{\tau} \tag{3}$$

We will focus on constitutive relations of this type, where the extra stress tensor is written in terms of the shear rate $\dot{\gamma}$ and the symmetric part of the velocity gradient

$$\boldsymbol{\tau} = 2\eta(\dot{\gamma})\mathbf{D}(\boldsymbol{u}) = \eta(\dot{\gamma})(\nabla \boldsymbol{u} + (\nabla \boldsymbol{u})^T). \tag{4}$$

Note that if η is a constant we recover the classical Navier–Stokes equations. In this work, since we aim at applications to hemodynamics, we use the Carreau-Yasuda viscosity model which fits experimental data (see [2] and references therein) and is given by

$$\eta(\dot{\gamma}) = \eta_\infty + (\eta_0 - \eta_\infty)\left[1 + (\lambda\dot{\gamma})^a\right]^{\frac{n-1}{a}}. \tag{5}$$

This is a five constants model where η_0 and η_∞ are the asymptotic viscosities at zero and infinite shear rates, λ is a time relaxation parameter, and a, n are parameters chosen to fit experiments (when $a = 2$ this is known as the Carreau model). When $n = 1$ or $a = 0$ or $\lambda = 0$ the viscosity is constant and the fluid behaves as Newtonian. For $n > 1$ the fluid is shear-thickening and for $n < 1$ it has shear-thinning behaviour. Figure 2 illustrates the viscosity behaviour for several values of the power index n.

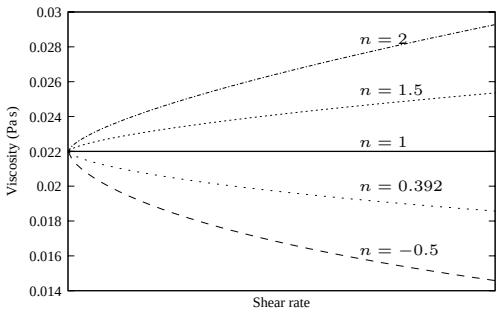

Figure 2: Viscosity vs. shear rate for the Carreau-Yasuda model, at different values of the power index ($n = 0.392$ corresponds to blood, see [2]).

2.2 Rigid body motion

The motion of B is said to be rigid if the velocity field over B can be written as

$$\boldsymbol{u}(\boldsymbol{x}) = \mathbf{U} + \omega \times (\boldsymbol{x} - \mathbf{G}), \qquad \text{on } \partial B_t \tag{6}$$

where ω and $\mathbf{U}$ are respectively the angular and translational velocities of B and $\mathbf{G}$ is a point in B, usually the center of mass. It can easily be shown that equation (6) is equivalent to

$$\nabla \boldsymbol{u} + (\nabla \boldsymbol{u})^T = 0, \qquad \text{on } \partial B_t \tag{7}$$

In order to couple the solid and fluid parts we must prescribe compatibility conditions that are basically instantaneous equilibria conditions for the forces in the fluid/body interface. Denoting by $\zeta(t)$ the position of the geometrical center of B_t, we must have

$$M\zeta''(t) = -\int_\gamma \boldsymbol{\sigma} \cdot \boldsymbol{n} + \int_{B_t} \boldsymbol{f}_b \tag{8}$$

$$J\omega'(t) = -\int_\gamma (\boldsymbol{x} - \zeta(t))^\perp \cdot \boldsymbol{\sigma}\boldsymbol{n} + \int_{B_t} (\boldsymbol{x} - \zeta(t))^\perp \boldsymbol{f}_b \tag{9}$$

where M and J are the (constant) mass and momentum of inertia of B_t, given by $M = \int_B \rho_b$ and

$J = \int_B = \rho_b |\boldsymbol{x} - \boldsymbol{x}_0|^2$, ρ_b is the density of the body and $\boldsymbol{f}_b$ are the external body forces exerted on B_t.

2.3 The coupled problem

The fully coupled fluid–rigid body interaction problem consists in finding $\boldsymbol{u}, p, \omega$ and $\mathbf{U}$ such that

$$\begin{cases} \rho_f \dfrac{D\boldsymbol{u}}{Dt} = \nabla \cdot \boldsymbol{\sigma} + \boldsymbol{f} & \\ & \text{in } \Omega_t \\ \boldsymbol{\sigma} = -p\,\mathbf{I} + \eta(\dot{\gamma})(\nabla \boldsymbol{u} + (\nabla \boldsymbol{u})^T) & \\ \nabla \cdot \boldsymbol{u} = 0 & \text{in } \Omega_t \\ \boldsymbol{u} = 0 & \text{on } \Gamma \\ \nabla \boldsymbol{u} + (\nabla \boldsymbol{u})^T = 0 & \text{on } \gamma \end{cases} \tag{10}$$

and the compatibility conditions (8) and (9) hold. We remark that the constitutive equation for the stress tensor does not need to be of this particular form and, as long as $\boldsymbol{\tau}$ can be computed, more complex fluids (e.g. viscoelastic fuids) can be considered without any changes in our method.

3 Weak formulation

Having in mind the discretization by finite elements, we write the problem in a variational form. Let us consider the function spaces $V = H_0^1(\mathcal{O})^2$ and $Q = \{q \in L^2(\mathcal{O}) : \int_\Omega q = 0\}$. Multiplying the fluid equations by test functions $\boldsymbol{v} \in V$ and $q \in Q$ and integrating by parts over Ω we obtain

$$\int_\Omega \rho_f \frac{D\boldsymbol{u}}{Dt} \cdot \boldsymbol{v} + \int_\Omega \boldsymbol{\tau} : \nabla \boldsymbol{v} - \int_\Omega p \nabla \cdot \boldsymbol{v} =$$

$$\int_\Omega \boldsymbol{f} \cdot \boldsymbol{v} + \int_{\partial\Omega} \boldsymbol{v} \cdot (\boldsymbol{\sigma} \cdot \mathbf{n}), \quad \forall \boldsymbol{v} \in V$$

$$\int_\Omega q \nabla \cdot \boldsymbol{u} = 0, \qquad \forall q \in Q$$

We now consider the space of rigid motions over B, $K_B = \{\boldsymbol{v} \in V : \nabla \boldsymbol{v} + (\nabla \boldsymbol{v})^T = 0, \text{ in } B\}$, take into account the compatibility and boundary conditions, and rewrite the variational formulation introduced above as follows:

for every $t > 0$, find $\boldsymbol{u} \in K_B$ and $p \in Q$:

$$\begin{cases} \displaystyle\int_{\mathcal{O}} \rho \frac{D\boldsymbol{u}}{Dt} \cdot \boldsymbol{v} + \int_{\mathcal{O}} \boldsymbol{\tau} : \nabla \boldsymbol{v} = & \\ \displaystyle\int_{\mathcal{O}} p \nabla \boldsymbol{v} + \int_{\mathcal{O}} \boldsymbol{v} \cdot \boldsymbol{f}, \quad \forall \boldsymbol{v} \in K_B & (11) \\ \displaystyle\int_{\mathcal{O}} q \nabla \boldsymbol{u} = 0, \quad \forall q \in Q & \end{cases}$$

where $\rho = \rho_f \chi_\Omega + \rho_b(1 - \chi_\Omega)$ and $\boldsymbol{f}$ is extended by zero outside B. We observe that formulation (11) does not contain any boundary terms.

4 Discrete problem

The method of characteristics is used to discretize the total time derivative. If we denote by $\mathbf{X}^n(x)$ the characteristic associated with $\boldsymbol{u}$ then, at each time step, the discretized problem reads:

find $\boldsymbol{u}^{n+1} \in K_{B^{n+1}}$ and $p \in L_0^2(\mathcal{O})$ such that:

$$\frac{1}{\Delta t} \int_{\mathcal{O}} \rho^{n+1} \boldsymbol{u}^{n+1} \cdot \boldsymbol{v} + \int_{\mathcal{O}} (\boldsymbol{\tau}^{n+1} : \nabla \boldsymbol{v} - p^{n+1} \nabla \cdot \boldsymbol{v}) =$$

$$\frac{1}{\Delta t} \int_{\mathcal{O}} (\rho^n \boldsymbol{u}^n) \circ \mathbf{X}^n \cdot \boldsymbol{v} + \int_{\mathcal{O}} \boldsymbol{f}^{n+1} \cdot \boldsymbol{v}, \quad \forall \boldsymbol{v} \in K_{B^{n+1}}$$

and

$$\int_{\mathcal{O}} q \nabla \cdot \boldsymbol{u}^{n+1} = 0, \quad \forall q \in Q$$

where, knowing $\boldsymbol{u}^n$, B^{n+1} is computed updating the position of B^n, i.e. B^{n+1} is the rigid body at time t_{n+1}. In fact, it is easier to use $\mathbf{U}^n$ and ω^n, that can be computed from $\boldsymbol{u}^n$. When B is a circle of radius r we have

$$U_i = \frac{1}{\pi r^2} \int_B u_i, \quad \omega = -\frac{2}{\pi r^4} \int_B (\boldsymbol{u} - \mathbf{U}) \times (\boldsymbol{x} - \mathbf{G}).$$

If we make no assumptions on the shape of the body, ω and $\mathbf{U}$ can still be computed by solving the linear system

$$\begin{cases} |B|\, U_1 + \alpha_2 \omega = \int_B u_1 \\ |B|\, U_2 - \alpha_1 \omega = \int_B u_2 \\ -\alpha_2 U_1 + \alpha_1 U_2 - \alpha_3 \omega = \beta \end{cases} \tag{12}$$

where $\alpha_1 = \int_B (x_1 - G_1)$, $\alpha_2 = \int_B (x_2 - G_2)$, $\alpha_3 = \int_b \|\boldsymbol{x} - \mathbf{G}\|^2$ and $\beta = \int_B ((x_1 - G_1)u_2 - (x_2 - G_2)u_1)$.

This problem is equivalent to the minimization over $K_{B^{n+1}}$ of the functional

$$J^n(\boldsymbol{v}) = \frac{1}{2\Delta t}\int_{\mathcal{O}} \rho^{n+1}\boldsymbol{v}^2 + \int_{\mathcal{O}} \boldsymbol{\tau}^{n+1} : \nabla \boldsymbol{v} - \frac{1}{\Delta t}\int_{\mathcal{O}} (\rho^n \boldsymbol{u}^n) \circ \mathbf{X} \cdot \boldsymbol{v} - \int_{\mathcal{O}} \boldsymbol{f}^{n+1} \cdot \boldsymbol{v}$$

and it will be solved within the theoretical framework presented in the next section. At each time step the problem must be discretized in space. This will be done using a standard finite element method based on a suitable meshing of the domain, that leads to the solution of a linear system.

5 Abstract penalty method

The weak formulation (11) is called constrained since the enforcement of rigid motion over B is embedded in the functional spaces. The penalization approach aims at relaxing this constraint which can be done in an abstract setting. We next summarize the main results introduced in [7].

Let V be a Hilbert space with inner product $(\cdot,\cdot)$, $a(\cdot,\cdot)$ a symmetric, bilinear continuous and coercive form and $\varphi \in V'$. Let us also define the functional $J(v) = \frac{1}{2}a(v,v) - \langle \varphi, v\rangle$.

Proposition 1 *Let K be a subspace of V. The constrained minimization problem*

$$(P)\begin{cases} \text{Find } u \in K \text{ such that} \\ J(u) = \inf\limits_{v\in K} J(v) \end{cases} \tag{13}$$

has a unique solution characterized by

$$a(u,v) = \langle \varphi, v\rangle, \qquad \forall v \in K \tag{14}$$

and the following estimate holds

$$|u| \le \frac{1}{\alpha}\|\varphi\|.$$

Consider now a bilinear, symmetric and positive form $b(\cdot,\cdot)$ such that $K = \{v \in V : b(v,v) = 0\}$. For all $\varepsilon > 0$ we consider the unconstrained minimization problem (P_ε) of the functional

$$J_\varepsilon(v) = J(v) + \frac{1}{\varepsilon}b(v,v),$$

that has also a unique solution $u^\varepsilon \in V$. The following result holds

Theorem 2 *The sequence (u^ε) of solutions of problem (P_ε) converges to the solution u of problem (P), in V.*

Sketch of the proof: If we write the variational formulation of (P_ε) and substitute v by u^ε, using the fact that $b(\cdot.\cdot)$ is a positive form together with Proposition 1, it can easily be shown that the sequence (u^ε) is bounded and therefore there is a subsequence converging to $z \in V$. On the other hand, since $J(u^\varepsilon) \le J_\varepsilon(u^\varepsilon) \le J_\varepsilon(u) = J(u)$ we also have $J(z) \le \liminf J(u^\varepsilon) \le J(u)$. In particular, since $J_\varepsilon(u^\varepsilon) \le J(u)$, we have

$$\frac{1}{\varepsilon}b(u^\varepsilon, u^\varepsilon) \le J(u) + \|\varphi\|_{V'}|u^\varepsilon| \le C \tag{15}$$

and therefore $b(u^\varepsilon, u^\varepsilon) \to 0$ which, together with $0 \le b(z,z) \le \liminf b(u^\varepsilon, u^\varepsilon)$ means that $z \in K$ (because $b(z,z) = 0$) and consequently $z = u$. The same argument can be applied to any convergent subsequence and so we prove weak convergence of u^ε to u. Proof of strong convergence is straightforward using the norm associated to the scalar product induced by $a(\cdot,\cdot)$.

Proposition 3 *Denoting by C and α the continuity and coercivity constants of $a(\cdot,\cdot)$, the following estimate holds,*

$$|u^\varepsilon - u| \le \sqrt{\frac{C}{\alpha}}dist(u^\varepsilon, K).$$

Only making further assumptions on $b(\cdot,\cdot)$ we can obtain a more usable error estimate for the penalized solution. The following proposition gives sufficient conditions for linear convergence.

Proposition 4 *If we further assume that $b(\cdot,\cdot)$ is of the form $b(u,v) = (\Psi u, \Psi v)$, with Ψ linear, continuous and with closed range over a Hilbert space Λ, there exists a constant $C > 0$ such that*

$$|u^\varepsilon - u| \le C\varepsilon.$$

5.1 Hyper-viscosity unconstrained formulation

The abstract penalty method already introduced can be applied to problem (11), recognizing that the space K_B is the kernel of the operator

$$b(\boldsymbol{u},\boldsymbol{v}) = \int_B (\nabla \boldsymbol{u} + (\nabla \boldsymbol{u})^T) : (\nabla \boldsymbol{v} + (\nabla \boldsymbol{v})^T)$$

Instead of solving (11) in the constrained space K_B, we will solve the penalized unconstrained problem

For every $t > 0$, find $\boldsymbol{u} \in K_B, p \in Q$:

$$\begin{aligned}\int_\Omega \rho \frac{D\boldsymbol{u}}{Dt} \cdot \boldsymbol{v} &= \int_\Omega (\boldsymbol{\tau} : \nabla \boldsymbol{v} + p \nabla \boldsymbol{v} + \boldsymbol{f} \cdot \boldsymbol{v}) \\ &- \frac{1}{\varepsilon} \int_B D\boldsymbol{u} : D\boldsymbol{v}, \quad \forall \boldsymbol{v} \in V \\ \int_\Omega q \nabla \boldsymbol{u} &= 0, \qquad \forall q \in Q\end{aligned}$$

that is equivalent to the unconstrained minimization of the functional

$$J^n_\varepsilon(\boldsymbol{v}) = J^n(\boldsymbol{v}) + \int_B D\boldsymbol{v} : D\boldsymbol{v}.$$

Convergence when $\varepsilon \to 0$ is guaranteed by Proposition 4. The main advantage of relaxing the rigid motion constraint is the possibility of using standard fluid solvers (with minor changes), avoiding heavy programming tasks. The name *hyper-viscosity* arises from the fact that, in the Newtonian case, the penalty term is the stiffness operator restricted to B and multiplied by a factor of $1/\varepsilon$. Since the leading coefficient of the global stiffness operator is the viscosity, the application of this method results in an increase of the viscosity over the B, by a factor of $1/\varepsilon$.

6 Numerical results

The hyper-viscosity method was implemented using a general finite element solver/programming language called *Freefem++* (see [4]). The code accepts arbitrary 2D geometries for the domain and the body. We will present a simple numerical simulation that tests the angular velocity reported by the method, which is the most sensitive unknown. The parameters used in the simulation are those appropriate to model blood: $\eta_0 = 0.022 Pa\ s$, $\eta_\infty = 0.0022\ Pa\, s$, $\lambda = 0.11\ s$, $a = 0.664$ and $n = 0.392$ (see e.g [2]). In this simulation the computational domain is a circle of radius 3 and the particle is a circle of unit radius, initially placed at the center of the domain.This is the 2D analog of flow between concentric cylinders. At time $t = 0$ the outer boundary is set to move at constant angular velocity. Due to the no-slip boundary condition, the fluid starts a rotating movement to follow the outer boundary, also inducing the motion of the particle. The particle is initially at rest and starts an increasingly faster rotation until it reaches a terminal angular speed $\omega < \omega_{wall}$, without any translation. In figure 3 we show the time evolution of ω for different values of the power index n. The stronger line corresponds to the Newtonian fluid ($n = 1$). Above this curve we find the curves obtained for shear-thickening fluids ($n > 1$) and below those obtained for shear-thinning fluids ($n < 1$).

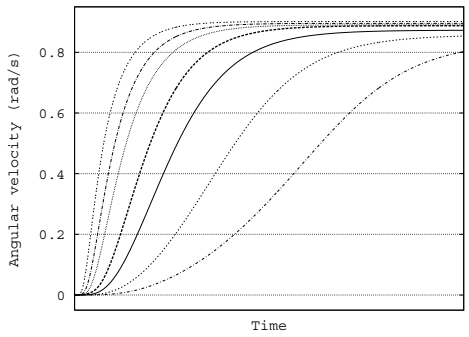

Figure 3: Angular velocity for several values of the power index ($n = 2.2,\ 1.8,\ 1.5,\ 1,\ 0.5,\ 0,\ -0.5$, from left to right)

We observe that for all values of the power index the same terminal angular velocity is achieved for the particle. However, the higher is the power index, the faster is the convergence. The curves in figure 3 can be used to design a simple Couette viscometer to identify the power index of the fluid.

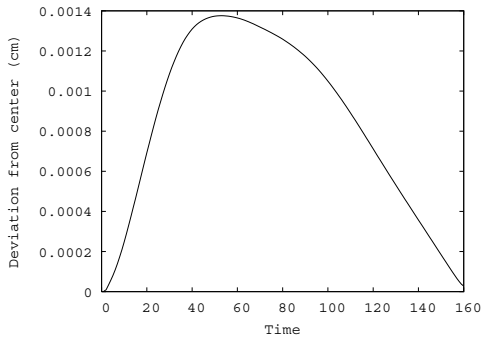

Figure 4: Distance from the center of the particle to the center of the domain.

In figure 4 we observe that, apart from rotating, the body also suffers a translation, describing a small orbit around the center of the domain which is due to numerical instabilities. This problem becomes relevant after a relatively large number of time steps, but can be arbitrarily delayed using finer meshes.
Finally figures 5 and 6 show some plots illustrating the evolution of the streamlines and shear-dependent viscosity, from the transient to the steady-state period. We observe that the streamlines initially concentrated near the outer boundary become equally distributed when the steady state is reached which is due to the constant angular velocity reached by the whole fluid. The same behaviour occurs with the shear-dependent viscosity.

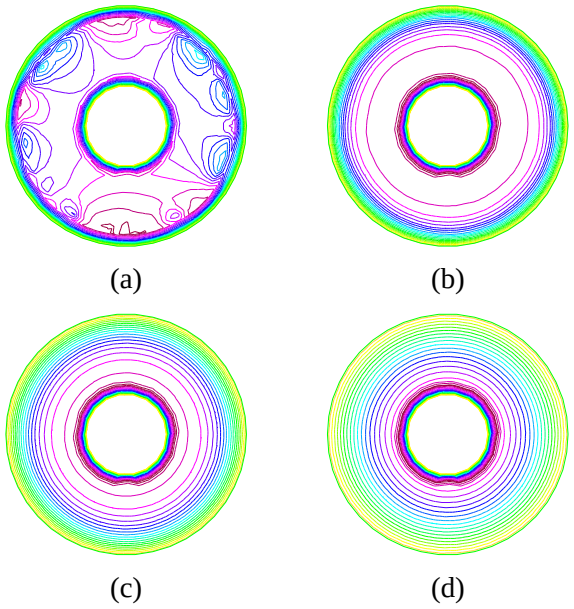

Figure 5: Evolution of the streamlines ($t = 0.1,\ 1.5,\ 4,\ 20\ s$).

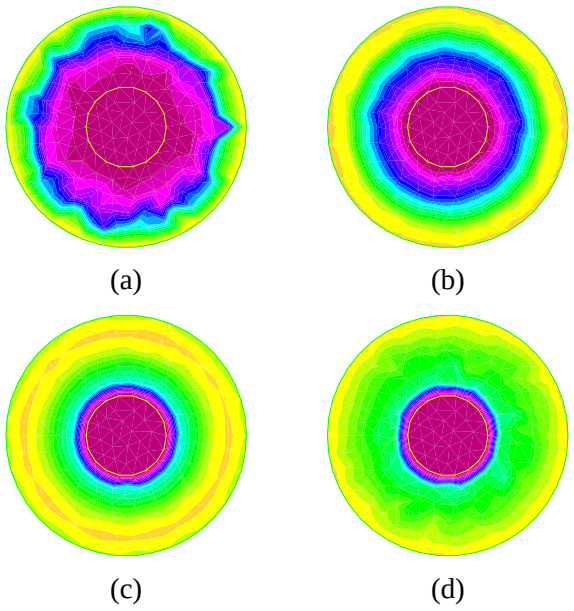

Figure 6: Evolution of the shear–dependent viscosity ($t = 0.1,\ 1.5,\ 4,\ 20\ s$).

7 Conclusions

A hyper-viscosity method has been derived and used to solve numerically fluid-rigid body interaction problems, in the case of a generalized Newtonian fluid. The convergence of the penalization procedure has been proved and numerical tests were carried out, showing differences between the Newtonian and non-Newtonian fluid behaviour related to the computation of the angular velocity.

The main advantage of this method is the possibility of using, with minor adaptations, widely available finite element packages and solvers for the Navier-Stokes equations.

Future work includes the derivation of sharp error estimates that can explain the observed rates of convergence and the extension of this method to viscoelastic models like Oldroyd-B or shear-dependent Oldroyd-B fluids.

Acknowledgements: We are grateful to Bertrand Maury for introducing this subject and to Aline Lefebvre for useful discussions. This work has been partially supported by the Center for Mathematics and its Applications - CEMAT through FCTs funding program and by the projects POCTI/MAT/41898/2001, POCTI/MAT/61792/2004 and HPRN-CT-2002-00270 (Research Training Network 'HaeMOdel' of the European Union).

References:

[1] R. Bai, R. Glowinski, D.D. Joseph and T.-W. Pan, Direct simulation of the motion of settling ellipsoids in a Newtonian fluid, *Proc. of the 14th Int.. Conf. on Domain Decomposition Methods*, 2002.

[2] F.J.H. Gijsen, E. Allanic, F.N. van de Vosse and J.D. Janssen, The influence of the non-Newtonian properties of blood on the flow in large arteries: unsteady flow in a 90 curved tube, *J. Biomech.* 32, 1999, pp. 705–713.

[3] P.Y. Huang, T. Ko, D.D. Joseph, and N.A. Patankar, Lift-off of a single particle in Newtonian and viscoelastic fluids by direct numerical simulation, *Journal of Fluid Mechanics*, 438, 2001, pp. 67-100.

[4] F. Hecht, A. Le Hyaric, O. Pironneau and K. Ohtsuka, *Freefem++ version 2.3-3*, http://www.freefem.org, 2006.

[5] J. Janela, A. Lefebvre and B. Maury, A penalty method for the simulation of fluid-rigid body interaction, *ESAIM Proceedings* 14, 2005, pp. 115–123.

[6] D.D. Joseph, Flow induced micro-structure in Newtonian and viscoelastic fluids, *Proc. of the 5th World Congress of Chem. Eng., Particle Technology Track*, AIChE, 6, 1996, pp. 3–16.

[7] B. Maury, Optimisation sous contrainte et méthode des éléments finis, *Université Paris-Sud* 2004.

[8] F.N. Van de Vosse et al., Finite–element–based computational methods for cardiovascular fluid–structure interaction, *Journal of Engineering Mathematics* 47, 2003, pp. 335–368.